Journal of Colloid and Interface Science 344 (2010) 10–20

Contents lists available at ScienceDirect

Journal of Colloid and Interface Science

www.elsevier.com/locate/jcis

Birefringent physical gels of *N*-(4-*n*-alkyloxybenzoyl)-L-alanine amphiphiles in organic solvents: The role of hydrogen-bonding

Trilochan Patra, Amrita Pal, Joykrishna Dey *

Department of Chemistry, Indian Institute of Technology, Kharagpur 721 302, India

ARTICLE INFO

Article history:
Received 15 August 2009
Accepted 2 December 2009
Available online 6 December 2009

Keywords:
Organogels
Amino acid-based amphiphiles
Hydrogen bonding
Microscopy
XRD
Rheology

ABSTRACT

A new class of amphiphiles, *N*-(4-*n*-alkyloxybenzoyl)-L-alanine was designed and synthesized. These amphiphiles have been shown to form thermoreversible gels in organic solvents such as aromatic hydrocarbons, cyclohexane, and chlorinated hydrocarbons at room temperature. The effects of amide functionality, chain length of the hydrocarbon tail, and the chirality of the head group of the amphiphiles on the ability to promote gelation in organic solvents have been studied. The *n*-tetradecyl derivative showed the best gelation ability, whereas the amphiphile with DL-alanine as the head group formed weak organogels. The 4-dodecyloxybenzoic-1-carboxyethyl ester derivative in which the amide group is replaced by an ester group also formed weak organogels at a slightly lower temperature (293 K). The gelation number and the gel melting temperature of the gelators in different solvents were determined. The rheological measurements suggested that the organogels of *n*-tetradecyl derivatives are stronger than those of amphiphiles containing *n*-dodecyl chains. Also the organogels of the amphiphiles, except the one with an ester group, were found to have gel-to-sol transition temperatures, T_{gs}, higher than room temperature (~303 K), which increased with the increase of chain length and total concentration of the gelator. SEM pictures of the gels show fibrous structures. Small-angle XRD and optical microscopy were also employed to characterize the gels. The organogels of alanine derivatives, except that of 4-dodecyloxybenzoic-1-carboxyethyl ester, showed optical birefringence. The mechanism of gelation was studied using ^{1}H NMR and FTIR spectroscopy. Hydrogen-bonding between $-CO_2H$ groups as well as π–π interactions were found to be important for the gelation process.

1. Introduction

Low-molecular-weight organogelators (LMOGs) that are used to harden organic liquids are of growing interest in the area of academic research in chemistry because of their potential for creating new soft materials, which may find applications in the environment, industry, and medicine [1–9]. Organogels are of great significance particularly for their potential uses as templates for material synthesis, drug delivery, cosmetics, separations, sensors, and biomimetics [10]. The gelator molecules organize themselves into supramolecular aggregates within the organic solvent, resulting in a three-dimensional structure, which causes the gelation. The three-dimensional (3-D) networks responsible for gelation are built by the noncovalent interactions among gelator molecules, such as hydrogen-bonding (H-bonding), hydrophobic interactions, van der Waals forces, π–π interactions, electrostatic interactions, and metal ion coordination [11–13]. It is also widely accepted that the ability to form gels is often associated with the presence of stereogenic centers in the molecular structures of LMOGs [14]. Indeed chirality plays critical roles in assembling processes taking place on surfaces and interfaces, in the liquid crystal phase, and in the formation of supramolecular polymers and gels [4,15]. In other words, the impact of chirality on assembled systems can be profound.

During the past 20 years a great deal of effort has been made to develop new types of LMOGs to understand the links between the properties and the structures of LMOGs and their organogels [16]. The LMOGs can be divided into two major groups—hydrogen bond-based gelators and non-hydrogen bond-based gelators. In amide compounds, such as amino acids [17–21] and urea [22–24], hydroxyl compounds, such as sugars [25–28], H-bonding is responsible for gelation. On the other hand, anthracene, cholesterol, and tropone derivatives [29–33] are non-hydrogen bond-based gelators. Amino acid–based gelators are mostly found to be biocompatible and biodegradable in nature. Recently, organogels of L-alanine derivatives have been shown to have potential applications in drug delivery [34,35]. It has been reported that *N*-acyl-L-alanine amphiphiles can gelate a number of hydrocarbon solvents, fuels [9,36,37], and sunflower oil [34]. Bhattacharya and co-workers [36] reported that the presence of both $-CO_2H$ and secondary amide (–NH–(=O)) groups is essential for the self-association of the amino acid-derived amphiphiles to form fibers, a necessary prerequisite for the

* Corresponding author. Fax: +91 3222 255303.
E-mail address: joydey@chem.iitkgp.ernet.in (J. Dey).

0021-9797/$ - see front matter © 2009 Elsevier Inc. All rights reserved.
doi:10.1016/j.jcis.2009.12.003

building of 3-D networks of organogels. On the other hand, the work of Motulsky et al. demonstrated the gelation of sunflower oil by methyl esters of *N*-acyl-L-alanine amphiphiles [34]. This means that only the amide H-bonding is important for gelation.

In order to further understand the nature of driving forces that self-assemble the amphiphiles to form fibers thus leading to gelation of organic solvents, we have designed and synthesized five new *N*-(4-*n*-alkyloxybenzoyl)-alanine amphiphiles, **1**–**5** (see Chart 1 for structures), and studied their gelling behaviors in different organic solvents. To examine the importance of the secondary amide group, we have also synthesized a structurally similar amphiphile, **6**, in which the amide group is replaced by an ester group. These amphiphiles contain a phenyl group in their alkyl chain, which can have either positive or negative effects on gelation. The present investigation was therefore undertaken to examine the role of a stereogenic center, and H-bonding and π–π interactions on the gelation ability of this class of amphiphilic molecules. We have employed a number of techniques, such as electron microscopy, polarizing optical microscopy, rheology, and XRD to characterize the organogels. ^{1}H NMR and FTIR spectroscopic techniques were used to study the nature of driving forces of gelation.

2. Materials and methods

2.1. Materials

Anhydrous potassium carbonate, sodium bicarbonate, 4-hydroxybenzoic acid, 1-bromododecane, 1-bromodecane, 1-bromooctane, *N*-hydroxysuccinimide (NHS), 1,3-dicyclohexylcarbodiimide (DCC), L-alanine, DL-alanine, and L-lactic acid were purchased from SRL, Mumbai, India, and were used without further purification. Tetrabutylammonium fluoride hydrate (TBAF), 1-bromohexadecane, and 1-bromotetradecane were obtained from Aldrich. All the organic solvents were of highest purity available and were dried and distilled fresh before use. The amphiphiles employed in this study were synthesized in the laboratory as described below.

2.2. Synthesis

The syntheses of *N*-[4-*n*-alkyloxybenzoyl]-L-alanine, -DL-alanine, and -L-lactic acid ester were carried out according to the procedure described elsewhere [38,39]. Briefly, 4-*n*-alkyloxybenzoic acid was first synthesized from 4-hydroxybenzoic acid and 1-bromoalkane and purified according to the reported procedure [40]. The coupling of L-alanine, DL-alanine, or L-lactic acid ester and 4-*n*-alkyloxybenzoic acid was made via the formation of NHS ester in the presence of DCC. Finally, the compound was purified by column chromatography using silica gel (60–120 mesh) as the column packing material. Chloroform was used to elute the impurities and ethyl acetate was used at the end to elute pure compound. Chemical identification of all the compounds was performed by use of ^{1}H NMR, elemental analysis, and FTIR spectroscopy (see ESI).

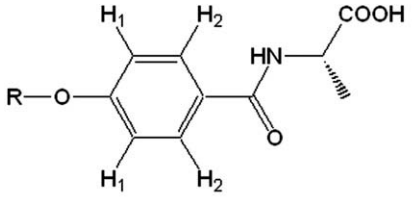

N-(4-n-alkyloxybenzoyl)-L-alanine

R = C_8H_{17} **[1]**, $C_{10}H_{21}$ **[2]**, $C_{12}H_{25}$ **[3a, 3b]**, $C_{14}H_{29}$ **[4]**, $C_{16}H_{33}$ **[5]**; L-alanine derivative, **1-5**, DL-alanine derivative, **3b**

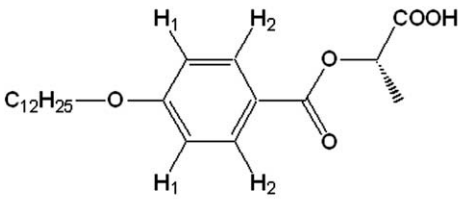

4-Dodecyloxy-benzoic acid 1-carboxy-ethyl ester **[6]**

Chart 1. Chemical structures of amphiphiles **1–6**.

2.3. Methods and instrumentation

FTIR spectra were measured with a Perkin–Elmer (Model Spectrum Rx I) spectrometer. ^{1}H NMR spectra were recorded on a Bruker 400 MHz instrument in $CDCl_3$ solvent with TMS as a standard. Melting point measurements were done using Instind (Kolkata) melting point apparatus with open capillaries. The measurements of optical rotations were performed with a JASCO (Model P-1020) digital polarimeter. The circular dichroism (CD) spectra were measured with a JASCO J-810 spectropolarimeter using a quartz cell with a path length of 1 mm. All measurements were done at room temperature (~303 K) unless otherwise noted.

The hot sample solution was placed on the aluminum or copper foil to make thin film and was left to cool and air dry at room temperature. The specimen after further overnight drying in desiccators was coated with gold particles to make a conducting surface and finally transferred into the field emission scanning electron microscope (FE-SEM, Zeiss, Supra-40) operating at 5–10 kV to obtain the micrographs. The polarizing optical light micrographs for the samples were obtained from a Leica-DM4500 optical microscope by transmitted light under crossed Nicol. The samples for optical microscopy contained gelators at a concentration less than the corresponding critical gelation concentration. A drop of the liquid was placed on the microscope slide and covered with a coverslip.

Wide-angle XRD (WAXRD) at a lower angular range was taken for all the air-dried gel samples (cast film on a glass slide) at room temperature. The experiment was performed on a Pan Analytica XPert Pro X-ray diffractometer using Cu target (Cu Kα) and Ni filter at a scanning rate of 0.001 s^{-1} between 2° and 10°, operating at a voltage of 40 kV, current 30 mA.

For all gels, rheological measurements in oscillatory mode were carried out on a Bohlin CVO D 100 controlled-stress rheometer using 20 mm diameter parallel plate geometry with a constant tool gap of 300 μm. The rheometer is fitted with a solvent trap and a peltier device that controls temperature within ±0.1 K. An equilibration time of 30 min was allowed before measurements were taken for each sample. All measurements were taken on matured gels after 10 h of cooling. Oscillatory stress sweeps from 0.1 to 1000 Pa (or 0.1 to 100 Pa) were measured at a constant frequency of 1 Hz to obtain storage modulus (G′) and loss modulus (G″). Prior to this a preliminary frequency sweep from 0.1 to 100 Hz was performed to determine the linear viscoelastic (LVE) regime. The shear strain (γ), phase angle (δ), dynamic viscosity (η^*), G′, and G″ were recorded as a function of time at a constant stress of 0.5 Pa that resulted in small strains (<0.2%).

3. Results and discussion

3.1. Gelation behavior of amphiphiles

The gelation of the amphiphiles **1**–**6** was tested in a variety of organic solvents including aliphatic hydrocarbons of varying chain length, chlorinated hydrocarbons, and aromatic hydrocarbons. All

the amphiphilic molecules remained either insoluble or crystallized out from straight chain hydrocarbon solvents on cooling to room temperature. Among the amphiphiles employed only compounds **3**–**5** showed gelation in cyclohexane, aromatic solvents, and chlorinated hydrocarbons at room temperature. The gelation occurred just by one or two alternate heating and cooling cycles. In a given solvent, gelation occurred when a critical concentration, called critical gelation concentration (CGC), of the gelator is reached. At room temperature and at gelator concentration close to CGC it took 3–5 h for the gelation to take place. However, the gelation time decreased drastically when gelator concentration was increased above CGC. It should be noted that for compound **3b**, it required about 12 h gelating solvents and the gel formed was weak and was not stable for a long time. The gel formation of the amphiphiles in organic solvents was tested by the "stable to inversion of the test tube" method (Fig. 1). Gelators **1** and **2** showed swelling and produced milky dispersion, respectively, in aromatic solvents. Compounds **3**–**6**, however, did not gel dichloromethane (DCM) solvent efficiently. This could be in part due to the high volatility of DCM, making the gelation process compete with evaporation. Compound **6** gels the aromatic solvents at slightly lower temperature (⩽293 K). The gelation behavior of the amphiphiles has been summarized in Table 1. It should be noted that the fatty acid derivatives of L-alanine formed transparent organogels in various acyclic hydrocarbon solvents [9,36,37]. But in the present work, the gel formed in most of the aromatic hydrocarbon solvents are opaque, whereas those formed in chlorinated solvents are translucent. Interestingly in nitrobenzene, the gel formed was transparent in contrast to the opaque optical nature of gels in other aromatic solvents. Thus an increase in optical clarity was observed on increasing the polarity of the aromatic solvent, which increases the solubility of the gelator. In most of the solvents, the gels remained unchanged for more than 2 months when preserved under a constant condition.

3.2. Influence of solvent on gelation

As recognized by many researchers the gelation of LMOGs in organic solvents is a consequence of gelator–gelator and gelator–solvent inter-molecular interactions of both specific and nonspecific nature [41,42]. The influence of these interactions can be understood by studying the effect of solvents on the gel formation. The gelation capability of a given gelator is not only relevant to the number and nature of solvents gelled by it, but also the minimum amount (CGC) of it needed to gel a given volume of solvent. For amphiphiles **3**–**6**, the CGC values (w/v %) (Table 1) were determined in various organic solvents. In most of the solvents employed, the CGC value of any gelator is high (>1%, w/v), which reflects its low gelating ability. Although the CGC value can be used to understand the influence of solvent, usually gelation number (defined as the number of moles of solvent gelled/number of moles of gelator) is correlated with solvent polarity parameter [41]. We have calculated gelation number using the CGC value of the amphiphiles at 298 K in different solvents and the data are listed in Table 2. The gelation numbers of these gelators are lower than those of the corresponding *N*-alkanoyl-L-alanine amphiphiles [36]. This can be attributed to the difference in gelator–solvent interaction for these two classes of gelators. Detailed discussion on the effect of gelator–solvent interactions on the gelation of organic solvents can be found elsewhere [41,42]. In the case of gelators **3**–**5**, the increased polarity of the hydrocarbon tail, which contains the phenoxy group, increases gelator–solvent interactions. This compromises the gelator–gelator H-bonding interactions responsible for gelator self-assembly, leading to reduced gelation numbers. The data in Table 2 suggest that in any given solvent, the gelation number increased as the hydrocarbon chain length increased up to C14. However, increase of chain length beyond C14 decreased the gelation number. This suggests that an optimum lipophilicity of the hydrocarbon tail of the gelator is required for efficient gelation.

Fig. 1. Photographs showing gelation of *p*-xylene solvent by the amphiphiles **3a** (a), **3b** (b), **4** (c), and **5** (d), and of nitrobenzene by **4** (f); gelation of *p*-xylene solvent by **4** (e) in the presence of TBAF (50 mol% of **4**).

Table 1
Results of gelation test for compounds **1**–**6**.

	Amphiphiles						
	1	**2**	**3a**	**3b**	**4**	**5**	**6**
Benzene	PG	MD	1.35	5.0	1.21	1.5	PG (3.88)
Toluene	C	MD	1.50	5.15	1.42	2.1	2.85 (2.50)
Chlorobenzene	PG	MD	1.32	5.35	1.10	1.27	PG (3.35)
Nitrobenzene	PG	MD	1.43	5.35	1.10	1.27	C
o-Xylene	PG	MD	1.65	4.55	1.54	1.7	PG (3.58)
p-Xylene	C	MD	1.40	3.85	1.30	1.75	3.05 (2.76)
m-Xylene	PG	MD	1.65	4.80	1.45	2.0	PG (3.35)
Mesitylene	PG	MD	1.58	3.50	1.12	1.67	PG (2.86)
Chloroform	S	S	2.85	MD	1.80	2.35	S
Tetrachloromethane	PG	MD	2.18	4.10	1.64	2.07	MD
n-Octane	I	I	I	I	I	I	I
n-Decane	I	I	MD	I	MD	I	I
Isooctane	I	I	I	I	I	I	I
Cyclohexane	C	MD	1.21	2.83	0.85	1.02	MD
Tetrahydrofuran	S	C	C	C	I	I	S
Carbon disulfide	S	S	PG	PG	PG	PG	PG

Values refer to the critical gelation concentration (CGC) (%, w/v) necessary for gelation at 298 K; C, crystallization; S, solution; I, insoluble; PG, partial gelation; MD, milky dispersion. Values within the parentheses represent CGC at 293 K.

Table 2
Gelation number (number of moles of solvent gelled/number of moles of gelator) of the amphiphiles **3**–**6** in different solvents at 298 K.

Solvents	**3a**	**3b**	**4**	**5**	**6**
Cyclohexane	288	69	359	333	–
Benzene	279	85	377	325	(110)
Toluene	237	69	268	247	125 (142)
Chlorobenzene	280	–	327	251	(111)
Nitrobenzene	257	56	423	139	–
o-Xylene	220	80	253	245	(101)
p-Xylene	218	80	253	200	100 (111)
m-Xylene	186	64	228	176	(92)
Mesitylene	172	77	260	186	(95)
Chloroform	166	–	283	231	–
Tetrachloromethane	179	96	256	217	–

Values within the parentheses represent gelation number at 293 K.

In other words, an optimum solubility of the amphiphiles is required for gelation to occur. Such lipophilic/lyophilic balance is well-known in the molecular assembly of biological membranes [43]. Perhaps lower solubility of C16 alkyl homologue results in formation of shorter fibers and hence decreases the ability to form 3-D network structures, which means a decrease of gelation number. This may be explained also by the partial tilt or bending of the C16 hydrocarbon chain, which weakens the gelator–gelator directional H-bonding forces, thereby reducing gelation number.

3.3. Influence of chirality

The role played by chirality in controlling and mediating the self-assembly of gelators is very important since many of the commonly employed LMOGs include chiral centers [15a]. The gelling ability of compound **3b**, which is the racemic form of **3a**, suggests that enantiomeric purity of the gelator is not required for gelation. However, the data in Table 2 show that the amphiphile **3b** has a gelation number much less than that of **3a**. This shows the importance of enantiomeric purity on the gelation ability of the amphiphiles. The organogel of **3b** was also found to be weaker and less stable than that of **3a**. Similar observations have also been made by Shinkai and co-workers who investigated a library of sugar-derived gelators and showed that different diastereomers have widely different gelation abilities [44]. In some cases, the racemic form of the gelator failed to gelate solvent [45,46]. On the other hand, Žinić and co-workers have reported an unusual example in which the racemic form of oxalamide gelator was found to be a

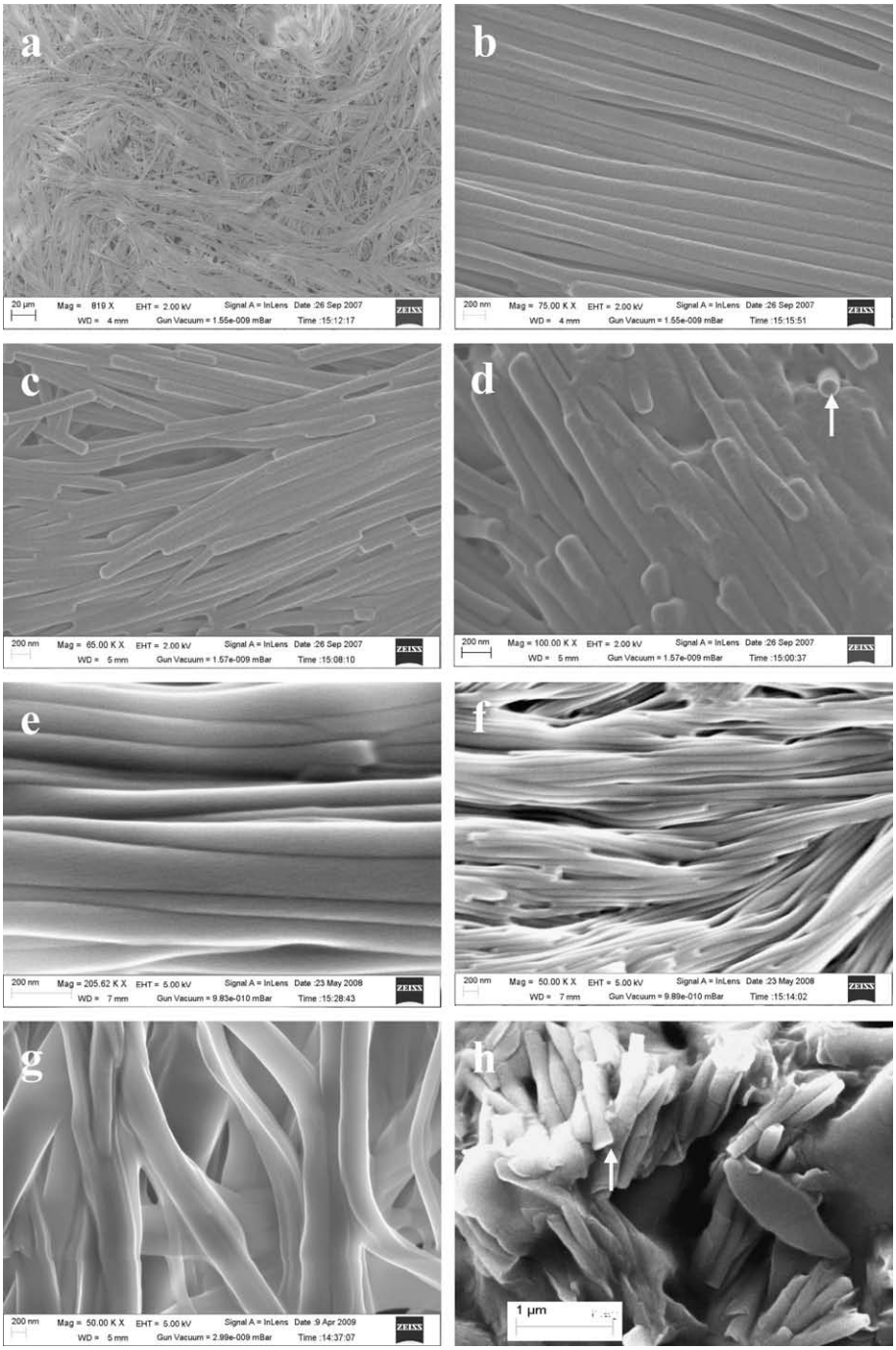

Fig. 2. FE-SEM images of *p*-xylene gels of (a, b) **3a** (2%, w/v), (c, d) **3b** (5%, w/v), (e) **4** (2%, w/v), (f) **5** (2%, w/v), and (g, h) **6** (5% w/v).

more efficient gelator than the individual enantiomers [47]. The chirality effects on the process of gel formation have been discussed in a review published by Huc and co-workers in 2005 [15a]. Indeed chirality has a significant role on the precisely organized inter-molecular interactions in gels. Homochiral interactions between alanine head groups of the gelators employed in this work perhaps facilitate one-dimensional (1-D) growth of the fibrous aggregates, the physical entanglement of which leads to the 3-D network structures. The more the entanglement, the higher the gelation number.

The homochiral interaction among chiral amphiphiles should lead to the formation of 1-D helical fibers, which can be confirmed by characteristic circular dichroism (CD) spectra. However, our attempt to measure CD spectra of the organogels of **3a** failed either because of the opacity of the gels or because of the strong absorption by the solvent (nitrobenzene) itself in the 200–280 nm range.

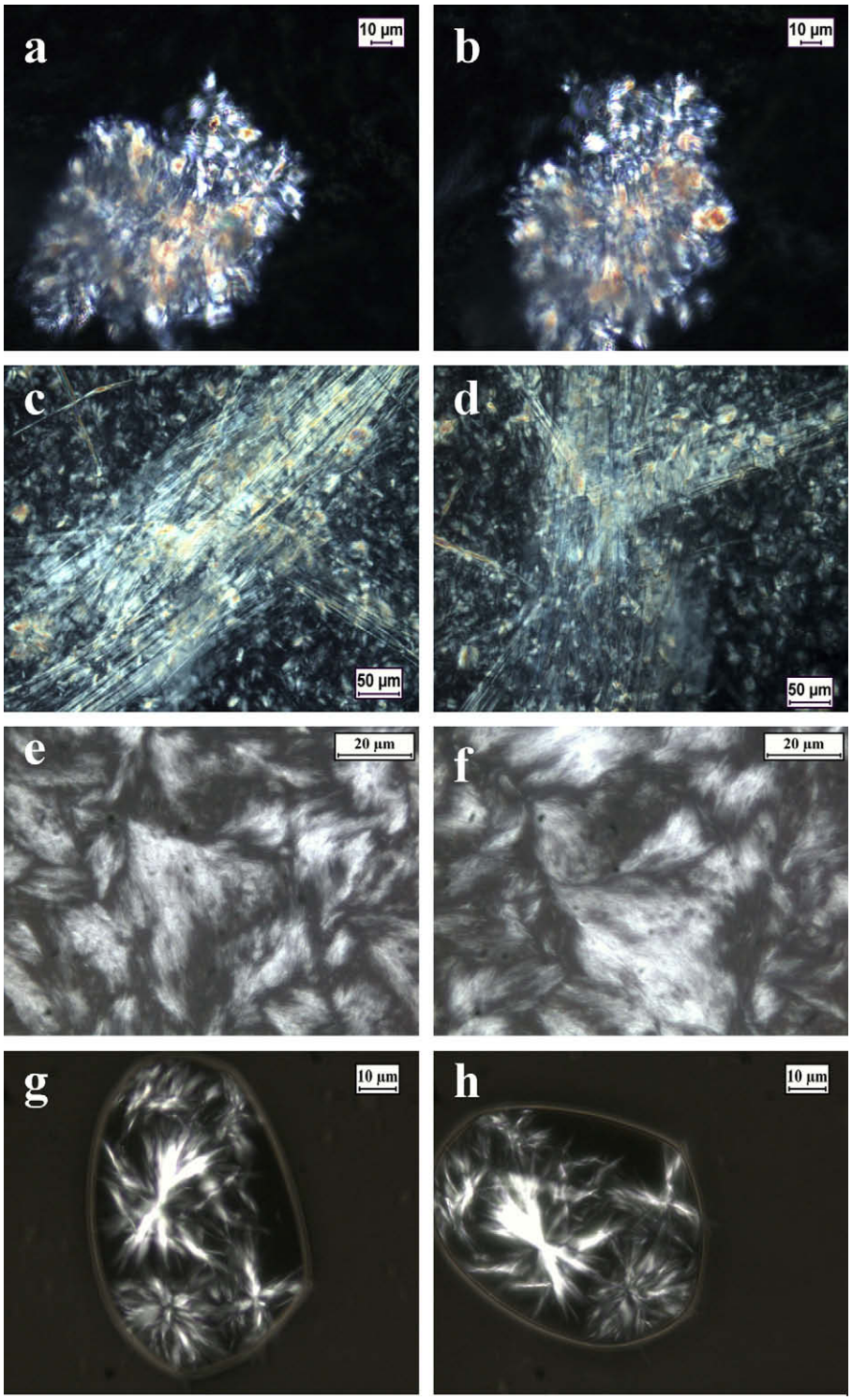

Fig. 3. Polarized optical micrographs of the organogels of **3a** (a, b), **3b** (c, d), **4** (e, f), and **6** (g, h) in *p*-xylene solvent at two different polarization angles (0° and 40°).

3.4. Morphology of the gels

As discussed above, chirality of the gelators is directly translated into the chirality of the gel fiber. In some gels, the chirality of the microstructures can be clearly visualized using SEM, TEM, or AFM techniques [14b,48,49]. Therefore, to obtain visual images of the gel aggregates of the amphiphiles in a given organic solvent, the morphology of the dry gels of **3a**, **3b**, **4**, **5**, and **6** was investigated by FE-SEM and optical microscopic techniques. The optical microscopic pictures (see Fig. S1 of ESI) clearly reveal the existence of fiber-like aggregates confirming the gel structure. The FE-SEM images of the gels in *p*-xylene solvent have been depicted in Fig. 2. The fiber-like 1-D aggregates of **3a** as shown in image 2a confirm gel formation and the experimental observations described above. The magnified FE-SEM images (Figs. 2b–h) of the dry gels of compounds **3a** and **3b** in *p*-xylene solvent clearly show that the amphiphiles are self-assembled into cylindrical aggregates of high aspect ratio, which accounts for the opacity of the organogels. The lengths of the cylinders are of the order of micrometers and their widths are about 50–100 nm and running parallel to each other without any cross linking among the fibers. In sample **3b**, since fracture occurred in a plane perpendicular to the axis of the cylinder (picture 2d) the cross-section can be seen (shown by arrow). The hollowness of the cylinders is clearly visible in the micrograph. The tubular structures of **3a** are very long but those of **3b** (picture 2c), which is structurally similar to **3a**, are only a few micrometers long. However, the micrographs of the gelators, **4** (image 2e), **5** (picture 2f), and **6** (image 2 g), reveal parallel lamellar sheets (ribbon-like aggregates). This kind of arrangement in molecular self-assemblies suggests some different properties, for example, liquid crystal (LC) behavior which is not very common among organogels.

It is interesting to observe that none of the above micrographs exhibits any helical aggregates. However, it should be noted that the morphologies present in a gel can be highly dependent on the method (for example, rate of cooling, sonication, etc.) used for gel formation. Since conventional SEM involves drying of the sample, morphological change can also occur during sample preparation. Also the SEM technique can only visualize fibers consisting of bundles of helical aggregates. It is also quite possible that a high degree of twist transforms the ribbon-like aggregates to tubules or rods as reported in the literature [50]. As seen in micrographs 2 g and h, the tubular structures can also be formed by rolling of lamellar structures like cigarette paper (shown by arrow). Thus the tubular structures in the micrographs are, perhaps, formed by this mechanism as no marks of twisting can be observed.

3.5. Polarizing optical microscopy

Optical anisotropy is an important property of LCs. Such anisotropy has been reported for organogelators forming rod-like assemblies [29,51]. According to a very classic case of organogels, it is well-known that the network structure formed by gelator molecules is crystalline in nature [15]. Optical micrographs of the fibrous gels of compound **3–6** in *p*-xylene solvent were therefore measured under crossed Nicols in transmitted mode. The polarized optical micrographs of representative samples are depicted in Fig. 3. Only the anisotropic organogels of **3a** and **3b** have strongly birefringent textures, revealing the presence of ordered structures. This indicates that the three-dimensional networks that are responsible for gelation contribute to the anisotropy. In the case of **3a** and **3b** nongeometric textures confirm hexagonal liquid crystal phases. This is consistent with the results of XRD and FE-SEM measurements, which as discussed above suggest that 3-D networks are constructed by the hexagonal phase. Surprisingly optical micrographs of the gels of compounds **4–6** were found to be very less or nonrefringent and generate a dark background (images 3e–h) under a polarizing microscope. Since gelators **4–6** are observed to form fibrous ribbons, their gels are expected to exhibit characteristic spherulite structures under polarized light as is typical for many chiral LC phases. However, generally polar solvents are required to observe such structures [52].

It is well-known that to exhibit mesomorphic properties it is desirable to have a rigid core and flexible alkyl side chains for the molecular design of LCs. The presence of a phenyl ring and a long hydrocarbon chain in the amphiphiles under study can fulfill these criteria. From FE-SEM images we found that the molecular self-assemblies in gel give parallel cylindrical or lamellar

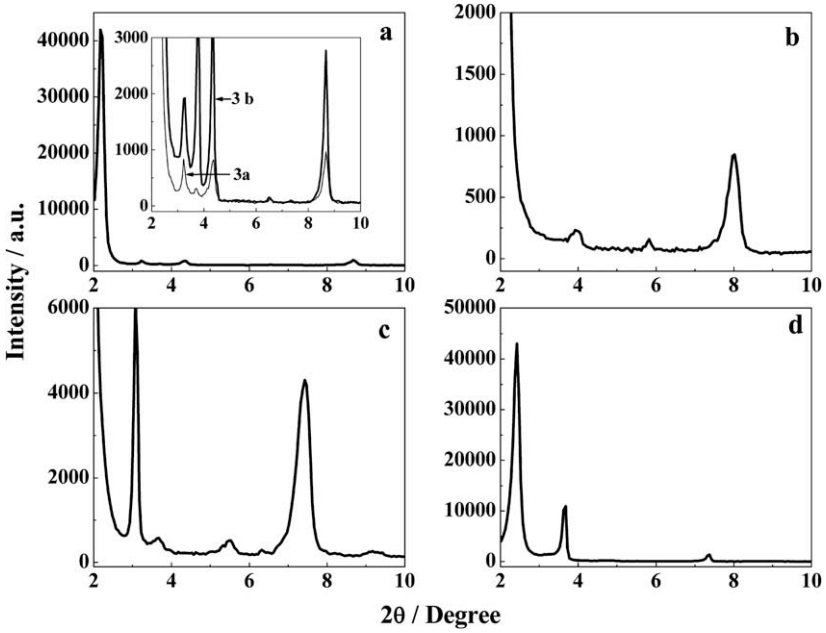

Fig. 4. X-ray diffraction patterns of a cast film from *p*-xylene gel of (a) **3a**, (2.5%, w/v); inset: magnified XRD spectra of **3a** and **3b** (5%, w/v), (b) **4**, (2.5%, w/v), (c) **5**, (2.5%, w/v), and (d) **6**, (5%, w/v).

structures. This suggests that these amphiphiles give either hexagonal or lamellar lyotropic LCs. An earlier report by Kubo et al. [29] has also shown gelation by rod-like LCs. A variety of liquid–crystalline materials have been prepared by self-assembly through H-bond formation [53,54]. It has been observed that gelators containing optically active acids and steroidal and condensed aromatic rings form lyotropic liquid crystal [55,56].

3.6. X-ray diffraction studies

The XRD patterns of the air-dried gel cast film of **3a** and **3b** in *p*-xylene solvent as representative examples have been depicted in Fig. 4. The peak positions (2θ values), corresponding planes, and inter-planar distances (d) have been included in Table S1 of Supporting information. The organogels of both **3a** and **3b** exhibit periodical diffraction peaks with their positions approximately at a ratio of $1:3^{1/2}:2:7^{1/2}$, which indicate that the molecules assemble into an ordered hexagonal structure [57]. On the other hand, the XRD spectra of the gels of **4**, **5**, and **6** exhibit peaks with positions at a ratio of 1:2:3, which suggest an ordered lamellar phase [58]. These peaks are due to the length of a repeat unit along the long axis of the molecule. The long spacing (d) corresponding to an intense and sharp diffraction peak at the small angle region of the XRD patterns of gelators **3**–**6** is almost twice that of the lipophilic segment. It is important to note that the position of the 100 peak shifted to lower 2θ values as the lipophilic segment of the gelators was increased, indicating a large increase of the aggregate size. In fact, for **4** and **5** with C14 and C16 chains, respectively, the 2θ value corresponding to the first 100 plane appeared at <2°. Interestingly, for gelators **3a**, **3b**, and **5** we observed aggregates of two different sizes.

3.7. Rheological behavior

Visual observation showed that the gels formed by these amphiphiles could not resist high mechanical force and break on shaking of the gel-containing vials. The rheological properties are important for the potential applications of the gels. The rheological behavior is strongly influenced by the superstructures, which form the network. For characterization of general rheological behavior and to provide information about the structure we have examined the organogels of **3a** and **4**. The results of the frequency sweep measurements are presented in Fig. 5. It can be found that for both organogels, G′ is always greater than G″ and both G′ and G″ show a very weak dependence of frequency in the LVE regime, which suggests that the samples are true gels. The G′/G″ ratio for the organogel of **4** is ca. 4.5, which is about twice that of **3a** (∼2.3). This means that the strength of the organogel of **4** is higher than that of **3a**. Fig. 6 shows the plots of G′ and G″ as a function of applied stress (σ). It is observed that each gel breaks down above a

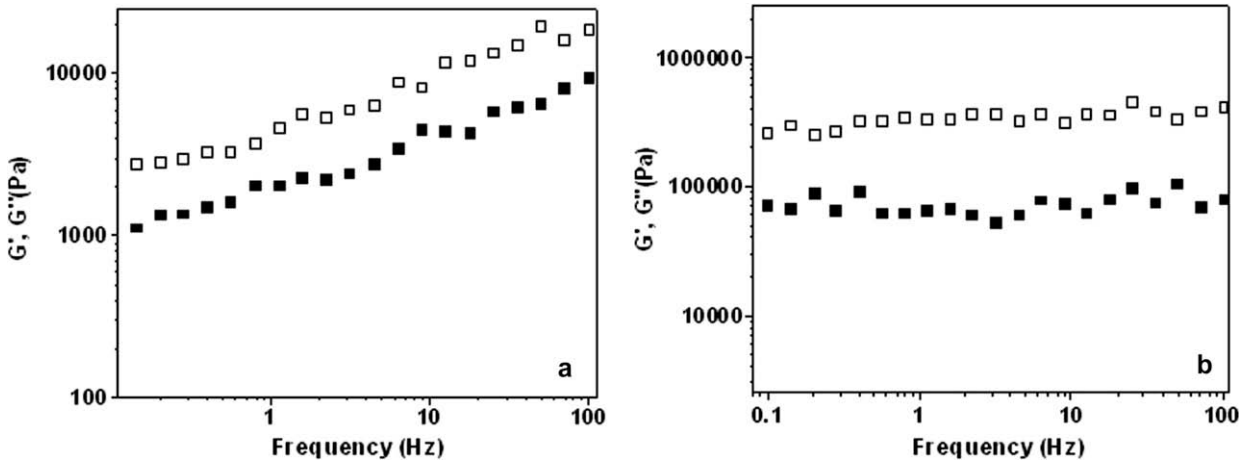

Fig. 5. Frequency (f) dependence of G′ (□) and G″ (■) of the organogels of (a) **3a** (5%, w/v) and (b) **4** (5% w/v) in *p*-xylene solvent at 298 K.

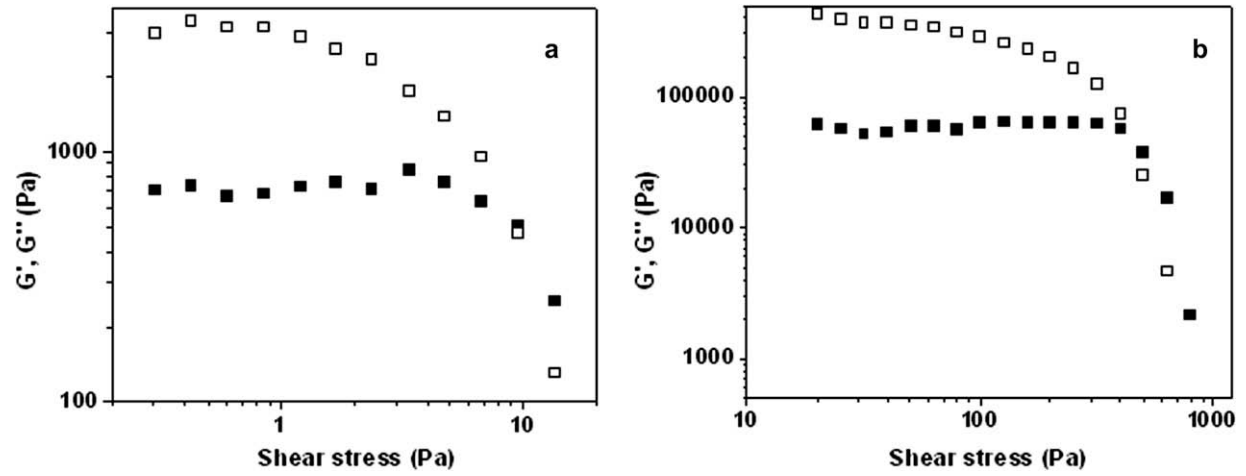

Fig. 6. Variation of G′ (□) and G″ (■) as a function of shear stress (σ) of the organogels of (a) **3a** (5%, w/v) and (b) **4** (5% w/v) in *p*-xylene solvent at 298 K.

so-called "yield stress" (σ_y) and begins to flow. The applied stress corresponding to the cross-section point of the two plots has been taken here as the yield stress. The σ_y values of the gels of **3a** and **4** are ca. 9 and ca. 435 Pa, respectively. The higher σ_y value of the organogel of **4** compared to that of **3a** indicates its greater strength. This can be attributed to the difference in microstructures of the organogels as shown by the FE-SEM images in Fig. 2. Indeed, the difference in aggregate morphology is confirmed by the XRD data as discussed in the preceding paragraph.

3.8. Gel-to-sol transition temperature

It has been noted earlier that organogels of the gelators employed in this work break on mechanical agitation, but are thermally quite stable. It is well established that gel formation is strongly dependent on the gelator concentration and temperature. Since higher gelator concentration promotes growth of self-assemblies, gelation is favored. On the other hand, higher temperature dismantles self-assemblies and thus disfavors gel formation. We have determined the gel melting temperature that is the gel-to-sol transition temperature (T_{gs}) of the organogels (Table 3) in three different solvents, keeping the gelator concentration fixed in each solvent. The gel melting temperature was determined by placing the screw cap glass vials containing gels in a temperature-controlled water bath and visually observing the flow on tilt for every degree rise in temperature. Although the gel structure was found to melt on heating, the gelation of the solution took place on cooling to room temperature. In other words, the gels are thermoreversible. The organogels, except that of **3b**, were found to have T_{gs} above 303 K. In any given solvent, T_{gs} was found to be highest for gelator **4**. The higher T_{gs} value for the organogel of **4** compared to that of **3a** is consistent with its greater yield stress value. It is interesting to observe that the organogel of **5** has a T_{gs} value lower than that of **4**. This is consistent with the higher CGC value of the former. The extent of physical entanglement of fibers is related to stability of the gel. More entanglement means higher stability and higher T_{gs} value. In the case of **5**, perhaps partial folding of the hydrocarbon chain hinders self-assembly formation and thus shortens the length of the fibers, thereby causing less entanglement. This is further indicated by the lower values of T_{gs} of gelators **3b** and **6** in which absence of homochiral and H-bonding interactions, as discussed above, causes reduction of the size of the self-assembled structures.

One of the important physical properties of gels is concentration-dependent gel–sol transition temperature. Increasing the concentration of the gelator is known to increase the thermal stability of the gel which means an increase of the T_{gs} value [59]. Therefore, for gelator **4**, we have also determined T_{gs} at different concentrations. As seen in Fig. 7, the T_{gs} value increases with increase in gelator concentration. It is interesting to note that although a nonlinear increase of T_{gs} can be observed for gels in both *p*-xylene and CCl_4 solvents, the nature of the curves is different. This must be due to the difference in interactions of the self-assembled aggregates with different solvent molecules.

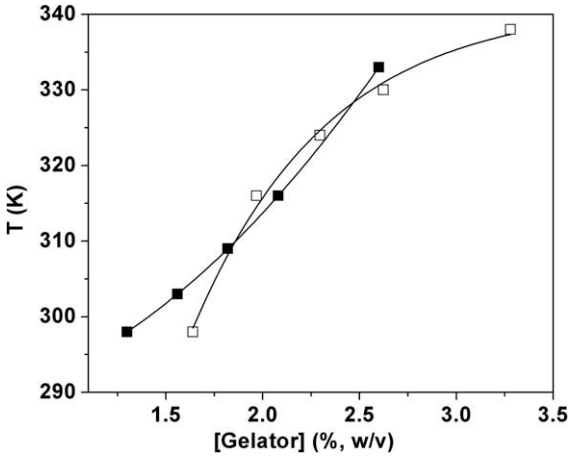

Fig. 7. Variation of T_{gs} with [gelator] for **4** in *p*-xylene (■) and CCl_4 (□) solvents.

3.9. Role of H-bonding in supramolecular aggregate formation

The gelation by compound **6** clearly suggests that the amide group is not necessary for self-assembly formation. However, the data in Table 2 show that gelation number of compound **6** is about one-half of that of **3a**. In the case of H-bonding gels, it is well established that the gelling efficiency of the gelators is either considerably reduced or the gel is completely destroyed by the addition of a small amount of compounds capable of forming H-bonds. In order to confirm H-bonding interaction of the $-CO_2H$ group we examined the gelation abilities of **3a** and **6** in *p*-xylene solvent in the presence of a small amount of TBAF (50 mol% of gelator). In both cases, gelation was not observed (see Fig. 1). This observation clearly indicates that the $-CO_2H$ group plays a crucial role in the self-assembly formation of the amphiphiles. It has been reported in the literature that the $-CO_2H$ group can promote gelation by inter-molecular H-bonding interactions [9]. However, apart from the $-CO_2H$ group the phenyl ring in the hydrocarbon chain of the amphiphiles may also contribute to self-assembly formation to some extent due to π–π-stacking interactions. In fact, the ability of **3**, **4**, and **5** to form gels in solvent like $CHCl_3$ suggests that π–π-stacking interactions among amphiphiles are also contributing to some extent in the formation of self-assemblies. Because H-bonding is significantly affected by the polarity and protic nature of the solvent as the acidic H of $CHCl_3$ always compete for the H-bonding. This is supported by the efficient gelation in CCl_4 in comparison with $CHCl_3$ as shown by the values of gelation numbers (Table 2).

FTIR spectra provide useful information on the state of H-bonds. Therefore, to further understand the roles of H-bonding in the process of gelation, FTIR spectra were recorded. The FTIR spectra of the solid (KBr pellet) compound **3a** and the dry gel in CCl_4 solvent were taken (Fig. S2 of ESI). The FTIR spectrum of **3a** in *p*-xylene showed a broad band around 3450 cm^{-1} revealing the presence of H-bonded OH groups in the gel state. The values of stretching frequencies of

Table 3
Gel melting temperature (T_{gs}, in K); values refer to the minimum temperature below which gelation occurs.

Amphiphiles	Solvent, concentration of amphiphiles (M)		
	p-Xylene, 0.102	Nitrobenzene, 0.0435	CCl_4, 0.063
3a	326	308	303
3b	298	–	–
4	345	325	328
5	343	319	326
6	306	–	–

Table 4
Comparisons of FTIR spectral data of **3a** and **6** in wet gel (CCl_4).

IR band	ν/cm^{-1}	
	3a	**6**
Amide A	3347 (3350)	–
Amide I	1635 (1636)	–
C=O of COOH	1707 (1708)	1718 (1736)
OH of COOH	3450 (3456)	3410 (3427)

Values within the parentheses represent respective stretching frequencies in powder (KBr) state.

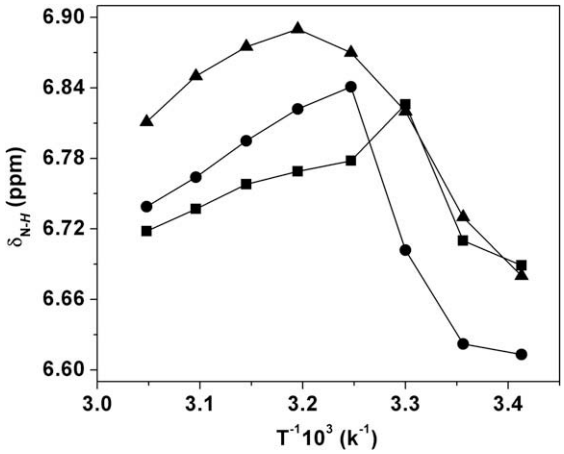

Fig. 8. Variation of chemical shift (δ_{N-H}) of amide proton with temperature in ^{1}H NMR spectra of the organogel of **4** (■) 1.65%, (●) 2%, (▲) 2.5% in CCl_4 and $CDCl_3$ (3:1, v/v) solvent.

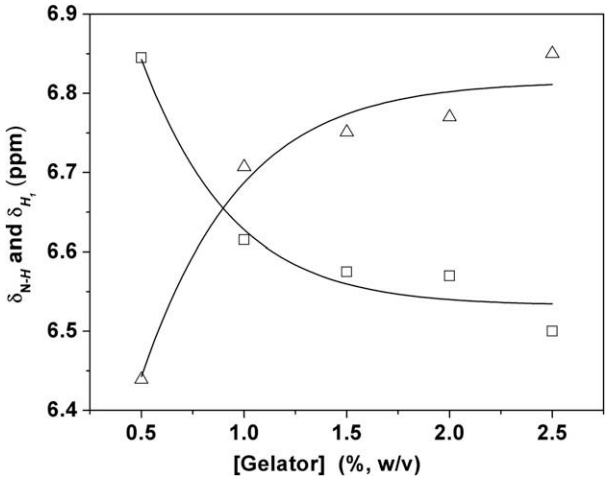

Fig. 9. Variation of chemical shift (δ) positions of the amide proton (Δ) and phenyl proton (Ph–H_1) (□) with gelator concentration in ^{1}H NMR spectra of the organogel of **4** in CCl_4–$CDCl_3$ mixture (3:1, v/v) at 323 K.

(–NH—C(=O)) and $-CO_2H$ group for both the gel and the solid compounds **3a** and **6** were compared with the stretching frequency values of non-hydrogen-bonded (–NH—C(=O)) and $-CO_2H$ groups (Table 4). The shift of the stretching frequencies to lower wavenumbers in the gel state suggests that both –NH—C(=O) and $-CO_2H$ groups in **3a** and $-CO_2H$ group in **6** are strongly H-bonded as they are in the solid state. Thus the most important factor controlling gelation seems to be H-bonding at the $-CO_2H$ sites.

Further, to determine the driving force for self-assembly formation of the gelators we have measured temperature- and concentration-dependent ^{1}H NMR spectra of the organogel of **4**. The ^{1}H NMR spectra of **4** (ca. 1.65% w/v, in CCl_4–$CDCl_3$ mixture (3:1, v/v)) in the temperature range 293–328 K are seen in Fig. S3 of ESI. The amide H-bonding and π–π-stacking interactions could be confirmed from the change in proton chemical shift (δ). The proton signal from the $-CO_2H$ group could not be observed, which might be due to strong >C=O···H—O H-bonding. However, the proton signal of the amide group (δ_{N-H}) of **4** at 293 K was found to be very weak. At 303 K, a broad signal at about 6.83 ppm assigned to the amide proton was detected. This implies that the inter-molecular H-bonds are formed between neighboring amide groups. The inter-molecular H-bond becomes weaker when the temperature is increased and as a result, the proton signal of the amide group is shifted upfield to 6.72 ppm at 328 K. The variation of δ_{N-H} value with temperature for amide proton is shown in Fig. 8. The initial downfield shift is due to strengthening of the H-bond, which becomes highest at 303 K. The signals of the aromatic protons δ_{H1}

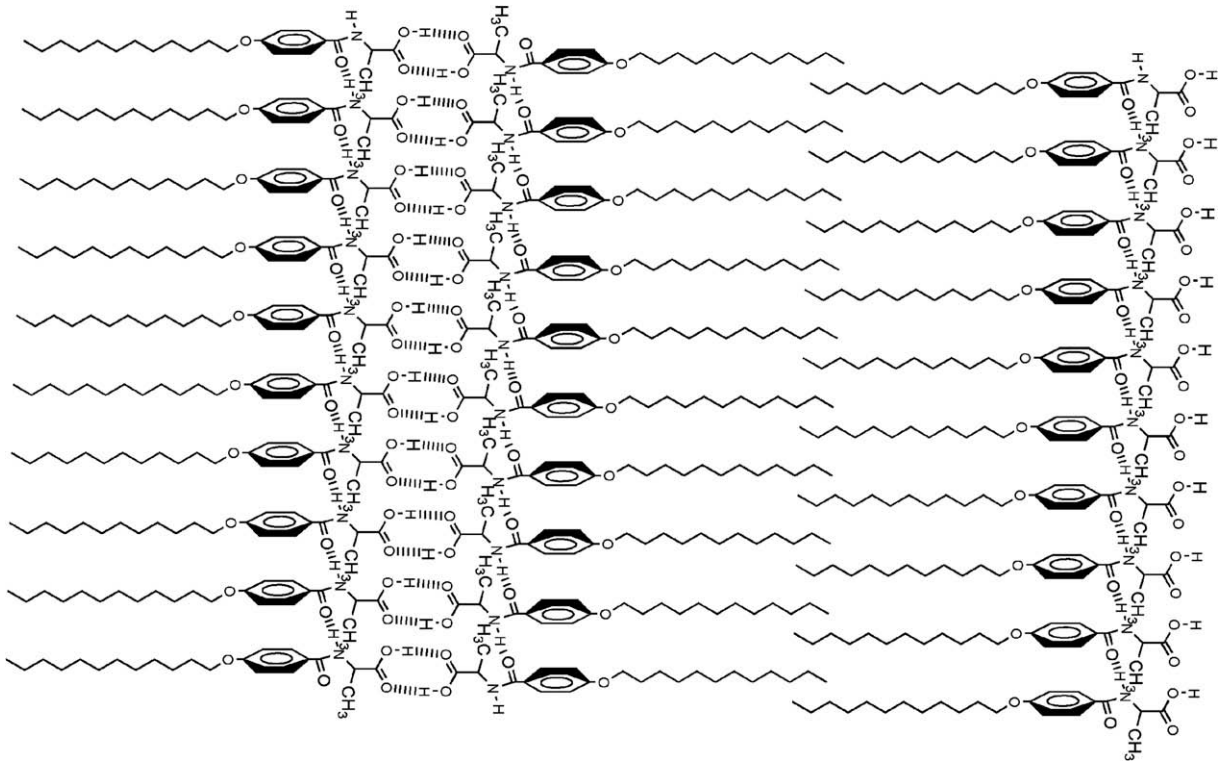

Fig. 10. Schematic representation of the local microstructure of the self-assembly in organogels.

and δ_{H2} in **4** were also found to be broad even at elevated temperatures. The signals shifted to lower field positions with the increase of temperature (Fig. S3 of ESI). The fall of δ_H value with the increase of temperature suggests a change in the microenvironment of amphiphiles due to loss of H-bonding and π–π-stacking interactions at higher temperatures. We also measured ^{1}H NMR spectra for different concentrations of **4** at 323 K (see Fig. S4 of ESI). The aromatic proton signals of concentrated solution (2.5% w/v) appeared at higher magnetic field (6.81 ppm) compared to that (6.87 ppm) in dilute solution (5 mg/mL) at the same temperature. A concentration-dependent shift of the signals of both amide (δ_{N-H}) and aromatic (δ_{H1}) protons was observed (Fig. 9). This chemical shift change of the aromatic protons with concentration implies π–π stacking among the benzene rings. This is also indicated by the relatively longer gelation time for the amphiphiles. In order to generate an optimized bilayer assembly and thereby to form a 3-D gel structure, the flat benzene ring in the lipophilic segment is positioned for π–π-stacking interactions which take longer time to attain. Thus from the XRD, FTIR, and ^{1}H NMR results it can be deduced that the gel aggregates consist of a repeating bilayer unit, which bears the head to head packing model (Fig. 10). Within the bilayer unit, the amphiphiles are connected by intra- and interlayer H-bonds to form an H-bond network to develop the super structures.

4. Conclusions

In summary, we have reported here the formation and properties of organogels formed by a series of alanine-based amphiphiles, *N*-(4-*n*-alkyloxybenzoyl)-L-alanine that bear an aliphatic chain linked to a phenyl ring. Among the amphiphiles, octyl and decyl derivatives do not show gelation, whereas dodecyl derivatives in both racemic and pure enantiomeric forms produce gels. In contrast to literature reports, chirality was found to be less important for gelator self-assembly formation and hence gelation, but optical purity of the gelator made the organogel stronger. Tetradecyl derivatives gelate with higher gelation number among all other amphiphiles. The dodecyl derivative was observed to gelate organic solvents even when the amide group was replaced by an ester group. This contrasts reported results that an amide group is essential for gelation. The presence of amide H-bonding, however, strengthens the organogel. Also, the results of rheological measurements showed that an optimum hydrocarbon chain length is required to produce stronger gels. The FTIR and ^{1}H NMR data clearly suggest that H-bonding at the head group (–CO_2H) and π–π stacking are necessary for the formation of bilayer self-assembly that produce gels. The physically weak organogels with lower gelation numbers are due to parallel arrangement of the gel fibers, implying a liquid crystal behavior of these compounds. The textures of the organogels with confined liquid crystal are birefringent, which confirms their optical anisotropy. The H-bonding between –CO_2H groups and π–π stacking are responsible for liquid crystal properties. Most of the stable organogels have T_{gs} above 303 K. The gelation process was observed to be thermoreversible. Thus the liquid crystalline organogels may find applications in drug delivery. Work in this direction is being carried out in this laboratory.

Acknowledgments

This work was financially supported by DST (Grant SR/S1/PC-18/2005), New Delhi, India. T.P. thanks CSIR (9/81(594)/2006-EMR-I) for a research fellowship.

Appendix A. Supplementary material

Supplementary data associated with this article can be found, in the online version, at doi:10.1016/j.jcis.2009.12.003.

References

[1] D.J. Abdallah, R.G. Weiss, Adv. Mater. 12 (2000) 1237–1247.
[2] Y.C. Lin, B. Kachar, R.G. Weiss, J. Am. Chem. Soc. 111 (1989) 5542–5551.
[3] K. Hanabusa, Y. Naka, T. Koyama, H. Shirai, J. Chem. Soc. Chem. Commun. (1994) 2683–2684.
[4] R. Oda, I. Huc, S.J. Candau, Angew. Chem. Int. Ed. 37 (1998) 2689–2691.
[5] (a) J.H. Jung, Y. Ono, K. Hanabusa, S. Shinkai, J. Am. Chem. Soc. 122 (2000) 5008–5009;
(b) J.H. Jung, Y. Ono, S. Shinkai, Angew. Chem. Int. Ed. 39 (2000) 1862–1865.
[6] J.H. Jung, M. Amaike, S. Shinkai, Chem. Commun. 23 (2000) 2343–2344.
[7] C.M. Garner, P. Terech, J.-J. Allegraud, B. Mistrot, P. Nguyen, D. de Geyer, A. Rivera, J. Chem. Soc., Faraday Trans. 94 (1998) 2173–2179.
[8] H.T. Stock, N.J. Turner, R. McCague, J. Chem. Soc. Chem. Commun. (1995) 2063–2064.
[9] S. Bhattacharya, A. Pal, J. Phys. Chem. B 112 (2008) 4918–4927.
[10] K. Kubo, A. Mori, Chem. Lett. 34 (2005) 1250–1251.
[11] J.H. Esch, B.L. Feringa, Angew. Chem. Int. Ed. 39 (2000) 2263–2268.
[12] P. Terech, R.G. Weiss, Chem. Rev. 97 (1997) 3133–3160.
[13] L.A. Estroff, A.D. Hamilton, Chem. Rev. 104 (2004) 1201–1218.
[14] (a) A. Friggeri, C. Pol, K.J.C van. Bommel, A. Heeres, M.C.A. Stuart, B.L. Feringa, J. van. Esch, Chem. Eur. J. 11 (2005) 5353–5361;
(b) J.H. Jung, Y. Ono, S. Shinkai, Chem. Eur. J. 6 (2000) 4552–4557;
(c) Y. Jeong, K. Hanabusa, H. Masunaga, I. Akiba, K. Miyoshi, S. Sakurai, K. Sakurai, Langmuir 21 (2005) 586–594.
[15] (a) A. Bizzard, R. Oda, I. Huc, Top. Curr. Chem. 256 (2005) 167–218;
(b) D. Berthier, T. Buffeteau, J. Lćger, R. Oda, I. Huc, J. Am. Chem. Soc. 124 (2002) 13486–13494.
[16] (a) M. George, G. Tan, V.T. John, R.G. Weiss, Chem. Eur. J. 11 (2005) 3243–3254;
(b) D.J. Abdallah, R.G. Weiss, J. Braz. Chem. Soc. 3 (2000) 209–218;
(c) A.R. Hirst, D.K. Smith, Chem. Eur. J. 11 (2005) 5496–5508;
(d) W.G. Weng, J.B. Beck, A.M. Jamieson, S.J. Rowan, J. Am. Chem. Soc. 128 (2005) 11663–11672.
[17] D. Khatua, J. Dey, Langmuir 21 (2005) 109–114.
[18] K.G. Ragunathan, S. Bhattacharya, Chem. Phys. Lipids 77 (1995) 13–23.
[19] K. Hanabusa, R. Tanaka, M. Suzuki, M. Kimura, H. Shirai, Adv. Mater. 9 (1997) 1095–1097.
[20] M. Suzuki, T. Sato, H. Shirai, K. Hanabusa, New J. Chem. 30 (2006) 1184–1191.
[21] J.G. Hardy, A.R. Hirst, I. Ashworth, C. Brennan, D.K. Smith, Tetrahedron 63 (2007) 7397–7406.
[22] J.V. Esch, S. DeFeyter, R.M. Kellogg, S. DeSchryver, B.L. Feringa, Chem. Eur. J. 3 (1997) 1238–1243.
[23] J.V. Esch, F. Schoonbeek, M. de Loos, H. Kooijman, A.L. Spek, R.M. Kellogg, B.L. Feringa, Chem. Eur. J. 5 (1999) 937–950.
[24] M. de Loos, J.V. Esch, R.M. Kellogg, B.L. Feringa, Angew. Chem. Int. Ed. 40 (2001) 613–616.
[25] N. Amanokura, K. Yoza, H. Shinmori, S. Shinkai, D.N. Reinhoudt, J. Chem. Soc., Perkin Trans. 2 (1998) 2585–2591.
[26] R.J.H. Hafkamp, M.C. Feiters, R.J.M. Nolte, J. Org. Chem. 64 (1999) 412–426.
[27] A. Srivastava, S. Ghorai, A. Bhattacharjya, S. Bhattacharya, J. Org. Chem. 70 (2005) 6574–6582.
[28] S. Bhattacharya, S.N.G. Acharya, Langmuir 16 (2000) 87–97.
[29] K. Kubo, K. Tsuji, A. Mori, S. Ujiie, J. Oleo Sci. 53 (2004) 467–470.
[30] R. Mukkamala, R. Weiss, Langmuir 12 (1996) 1474–1482.
[31] C. Geiger, M. Stanesau, L. Chen, D.G. Whitten, Langmuir 15 (1999) 2241–2245.
[32] L. Lu, T.M. Cocker, R.E. Bachman, R.G. Weiss, Langmuir 16 (2000) 20–34.
[33] J.H. Jung, H. Kobayashi, M. Masuda, T. Shimizu, S. Shinkai, J. Am. Chem. Soc. 123 (2001) 8785–8789.
[34] A. Motulsky, M. Lafleur, A.-C. Couffin-Hoarau, D. Hoarau, F. Boury, J.-P. Benoit, J.-C. Leroux, Biomaterials 26 (2005) 6242–6253.
[35] A.C. Couffin-Hoarau, P.D. Motulsky, J.C. Leroux, Pharm. Res. 21 (2004) 454–457.
[36] (a) S. Bhattacharya, Y.K. Ghosh, Chem. Commun. (2001) 185–186;
(b) A. Pal, Y.K. Ghosh, S. Bhattacharya, Tetrahedron 63 (2007) 7334–7348.
[37] X. Luo, B. Liu, Y. liang, Chem. Commun. (2001) 1556–1557.
[38] A. Mohanty, J. Dey, Chem. Commun. 12 (2003) 1384–1385.
[39] A. Mohanty, J. Dey, Langmuir 20 (2004) 8452–8459.
[40] S. Bhattacharya, M. Subramanian, U.S. Hiremath, Chem. Phys. Lipids 78 (1995) 177–188.
[41] G. Zhu, J.S. Dordick, Chem. Mater. 18 (2006) 5988–5995.
[42] R. Wang, C. Geiger, L. Chen, B. Swanson, D.G. Whitten, J. Am. Chem. Soc. 122 (2000) 2399–2400.
[43] R.B. Gennis, Biomembranes: Molecular Structure and Function, Springer Verlag, New York, 1989.
[44] O. Gronwald, S. Shinkai, Chem. Eur. J. 7 (2001) 4328–4334.
[45] J.-H. Fuhrhop, P. Schnieder, J. Rosenberg, E. Boekema, J. Am. Chem. Soc. 109 (1987) 3387–3390.

[46] J. Becerril, B. Escuder, J.F. Miravet, R. Gavara, S.V. Luis, Eur. J. Org. Chem. 3 (2005) 481–485.
[47] J. Makarević, M. Jokić, Z. Raza, Z. Štefanić, B. Kojić-Prodić, M. Žinić, Chem. Eur. J. 9 (2003) 5567–5580.
[48] K. Koumoto, T. Yamashita, T. Kimura, R. Luboradziki, S. Shinkai, Nanotechnology 12 (2001) 25–31.
[49] A. Ajayaghosh, V.K. Praveen, Acc. Chem. Res. 40 (2007) 644–656.
[50] J.H. Jung, S.H. Lee, J.S. Yoo, K. Yoshida, T. Shimizu, S. Shinkai, Chem. Eur. J. 9 (2003) 5307–5313.
[51] P. Terech, G. Gebel, R. Ramasseul, Langmuir 12 (1996) 4321–4323.
[52] G. Wang, A.D. Hamilton, Chem. Eur. J. 8 (2002) 1954–1961.
[53] T. Kato, N. Mizoshita, K. Kishimoto, Angew. Chem. Int. Ed. 45 (2006) 38–68.
[54] C.M. Paleos, D. Tsiourvas, Liq. Cryst. 28 (2001) 1127–1161.
[55] K. Sakamoto, R. Yoshida, M. Hatano, T. Tachibana, J. Am. Chem. Soc. 100 (1978) 6898–6902.
[56] D. Demus, L. Richter, Textures of Liquid Crystals, Verlag Chemie, Veinheim, 1978.
[57] (a) B. Kenta, C.J. Garveyb, D. Cooksonc, G. Bryanta, Chem. Phys. Lipids 157 (2009) 56–60;
(b) L. Cui, L. Zhu, Langmuir 22 (2006) 5982–5985.
[58] D. Kim, D. Sohn, J.Y. Kim, S. Lee, Y.K. Han, Polym. Preprints 42 (2001) 310.
[59] H. Kobayashi, A. Friggeri, K. Koumoto, M. Amaike, S. Shinkai, D.N. Reinhoudt, Org. Lett. 4 (2002) 1423–1426.